Progress In Electromagnetics Research M, Vol. 66, 99–107, 2018

A Novel Method for Cogging Torque Reduction in Permanent Magnet Brushless DC Motor Using T-shaped Bifurcation in Stator Teeth

M. Arun Noyal Doss*, R. Brindha, K. Mohanraj, Shubranshu S. Dash, and K. M. Kavya

Abstract—A variety of techniques are available to reduce cogging torque in Permanent Magnet Brushless DC (PMBLDC) motors. In general, all the techniques are meant for effectively reducing the cogging torque. This paper presents a new technique for cogging torque reduction in a radial flux surface mounted PMBLDC motor by applying the proposed T-shaped bifurcation method in the stator teeth of a PMBLDC motor. The Finite Element Analysis (FEA) is carried out for the T-shaped bifurcation method applied to a PMBLDC motor, and analysis is done using Virtual Work (VW) method. The CAD software package MagNet has been used to completely analyze the T-shaped bifurcation based PMBLDC motor. FEA and CAD simulated results are compared for the reduction of cogging torque values. It is found that the cogging torque reductions in the two methods are nearly the same. The cogging torque and the flux density values of the motor calculated using the proposed T-shaped bifurcation method are compared with the corresponding values of the recently introduced Reduced Stator Slot Width method. The proposed T-shaped bifurcation is very effective compared to the existing techniques in reducing the cogging torque.

1. INTRODUCTION

Permanent Magnet Brushless DC (PMBLDC) motor has been widely used for high performance applications in industrial drives due to its various special features such as high torque density, high reliability, high power factor and low acoustic noise. Cogging torque is one of the most important causes affecting the performance of PMBLDC motors. Cogging torque minimization has become an important issue since the motor has to improve its performance for torque ripple sensitive applications such as electric power steering and robotics. Several experimental researches have been carried out in cogging torque minimization [1–12]. The T-shape bifurcation shows good impact on reducing cogging torque compared with reduced stator tooth techniques, which was an effective technique in stator slot modification technique. This technique is applied in stator teeth and creating a auxiliary slot in the teeth.

In this paper, the analysis of T-shaped bifurcation to reduce the cogging torque is carried out by analytical techniques. The Virtual Work (VM) method is combined with Finite Element Analysis to evaluate the cogging torque and to show that the T-shaped bifurcation method is very effective in cogging torque minimization. The analytical and CAD simulated results are compared for cogging torque reduction in T-shape bifurcation in stator teeth.

Received 9 November 2017, Accepted 6 February 2018, Scheduled 27 March 2018
* Corresponding author: M. Arun Noyal Doss (arunnoyal@gmail.com).
The authors are with the Department of Electrical and Electronics Engineering, SRM University, India.

2. ANALYSIS OF COGGING TORQUE

Cogging torque occurs in PM motors in the air gap between rotor and stator. The interaction between the stator slots and rotor magnets is called cogging torque. It is the energy variation within a motor when there is no current in the windings. As the rotor starts rotating, the reluctance in the air gap changes. The path of the magnetic flux exits from magnets to rotor, and then follows through the air gap and stator; lastly it returns to the magnets. The reluctance in the air gap is different from the reluctances in the rotor and stator. Figure 1 shows the schematic representation of a PMBLDC motor. The cogging torque is formed in the air gap as a force and can be calculated from the stored energy in the air gap. This cogging torque is calculated using the Virtual Work Method (VWM) as shown below.

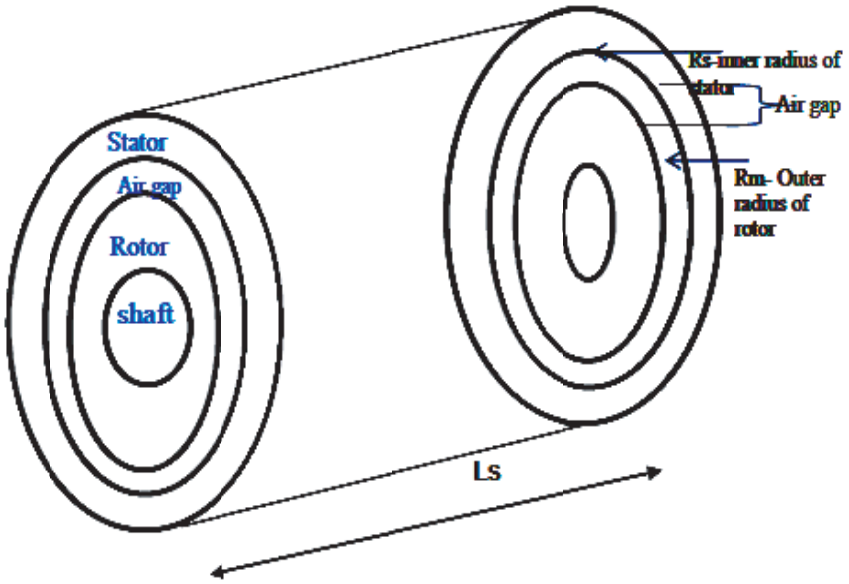

Figure 1. Schematic representation of a PMBLDC motor.

The cogging torque (T_{cog}) is given by

$$T_{cog} = -\frac{\partial W(\alpha)}{\partial \alpha} \tag{1}$$

where W is the stored energy in the air gap, and α is the position angle of the rotor.

For surface mounted permanent magnet type of BLDC motor, the stored energy in the air gap (W) is given by

$$W(\alpha) = \frac{1}{2\mu_o} \int_v (F(\theta, \alpha) \cdot P(\theta))^2 dv \tag{2}$$

$$F(\theta, \alpha) = \frac{g}{\mu_o} \cdot B(\theta, \alpha) \tag{3}$$

$$P(\theta) = \frac{\mu_o}{g} \cdot G(\theta) \tag{4}$$

In the above $F(\theta, \alpha)$ is the air gap magneto motive force function, and $P(\theta)$ is the air gap permeance function.

Substituting Eqs. (3) and (4) in Eq. (2)

$$= \frac{1}{2\mu_o} \int_v (B(\theta, \alpha) \cdot G(\theta))^2 dv$$

$$
\begin{aligned}
&= \frac{1}{2\mu_o} \int_0^{L_s} \int_{R_m}^{R_s} \int_0^{2\pi} (B(\theta,\alpha)\cdot G(\theta))^2 d\theta \cdot r dr \cdot dz \\
&= \frac{1}{2\mu_o} \int_0^{L_s} dz \int_{R_m}^{R_s} r dr \int_0^{2\pi} (B(\theta,\alpha)\cdot G(\theta))^2 d\theta \\
&= \frac{1}{2\mu_o} [z]_0^{L_s} \left[\frac{r^2}{2}\right]_{R_m}^{R_s} \int_0^{2\pi} (B(\theta,\alpha)\cdot G(\theta))^2 d\theta \\
&= \frac{L_s}{4\mu_o} \left[R_s^2 - R_m^2\right] \int_0^{2\pi} (B(\theta,\alpha)\cdot G(\theta))^2 d\theta \qquad (5)
\end{aligned}
$$

From Eq. (5), $B(\theta,\alpha)^2$ and $G(\theta)^2$ can be calculated through Fourier series expansions and are given below.

$$B(\theta,\alpha)^2 = \sum_{n=0}^{\infty} B_{nN_P} \left(\cos(nN_P(\theta-\alpha)) + \sin(nN_P(\theta-\alpha))\right) \qquad (6)$$

$$G(\theta)^2 = \sum_{n=0}^{\infty} G_{nN_s} \left(\cos(nN_s\theta) + \sin(nN_s\theta)\right) \qquad (7)$$

where L_s is the length of stator and rotor, B the Flux density, G the relative air gap permeance function, R_m the outer radius of Rotor, R_s the inner radius of Stator, N_P the number of rotor poles, and N_s the number of Stator slots.

Substituting Eqs. (6) and (7) in Eq. (5)

$$W(\alpha) = \frac{L_s}{4\mu_o}(R_s^2 - R_m^2) \int_0^{2\pi} \sum_{n=0}^{\infty} B_{nN_s} \begin{pmatrix} \cos(nN_P(\theta-\alpha)) \\ +\sin(nN_P(\theta-\alpha)) \end{pmatrix} \cdot G_{nN_s} \begin{pmatrix} \cos(nN_s\theta) \\ +\sin(nN_s\theta) \end{pmatrix} d\theta \qquad (8)$$

Replace N_p and N_s by N_L (which is the least common multiple (LCM) between N_p and N_s), and hence N_L is given by

$$N_L = LCM(NP, NS)$$

It is obvious that for symmetric motors the sine terms are zero.

Hence,

$$W(\alpha) = \frac{L_s}{4\mu_o}(R_s^2 - R_m^2) \int_0^{2\pi} \sum_{n=0}^{\infty} B_{nN_L} G_{nN_L} \cos(nN_L(\theta-\alpha)) \cdot (\cos nN_L\theta)\, d\theta$$

In the above equation

$$
\begin{aligned}
\cos(nN_L(\theta-\alpha)) \cdot \cos(nN_L\theta) &= \frac{1}{2}\cos(nN_L(\theta-\alpha) + nN_L\theta) + \cos(nN_L(\theta-\alpha) - nN_L\theta) \\
&= \frac{1}{2}\cos(nN_L\theta - nN_L\alpha + nN_L\theta) + \cos(nN_L\theta - nN_L\alpha - nN_L\theta) \\
&= \frac{1}{2}\cos(2nN_L\theta - nN_L\alpha) - \cos(nN_L\alpha)
\end{aligned}
$$

Continuing the evaluation of above equation $W(\alpha)$,

$$W(\alpha) = \frac{L_s}{4\mu_o}(R_s^2 - R_m^2) \int_0^{2\pi} \sum_{n=0}^{\infty} B_{nN_L} G_{nN_L} \cdot \frac{1}{2}\cos(2nN_L\theta - nN_L\alpha) - \cos(nN_L\alpha) \cdot d\theta$$

$$= \frac{L_s}{4\mu_o}(R_s^2 - R_m^2)\sum_{n=0}^{\infty} B_{nN_L}G_{nN_L}\int_0^{2\pi}\frac{1}{2}\cdot(-\cos(nN_L\alpha)+\cos(2nN_L\theta - nN_L\alpha))\cdot d\theta$$

$$= \frac{L_s}{4\mu_o}(R_s^2 - R_m^2)\sum_{n=0}^{\infty} B_{nN_L}G_{nN_L}\left(\frac{-\cos(nN_L\alpha)}{2}\cdot\int_0^{2\pi} d\theta + \int_0^{2\pi}\frac{\cos(2nN_L\theta - nN_L\alpha)}{2}\right)\cdot d\theta$$

$$= \frac{L_s}{4\mu_o}(R_s^2 - R_m^2)\sum_{n=0}^{\infty} B_{nN_L}G_{nN_L}\left(-\frac{\cos(nN_L\alpha)}{2}[\theta]_0^{2\pi} + \int_0^{2\pi}\frac{1}{2}\begin{pmatrix}\cos(2nN_L\theta)\cdot\cos(nN_L\alpha)\\ +\sin(2nN_L\theta)\cdot\sin(nN_L\alpha)\end{pmatrix}\cdot d\theta\right)$$

$$= \frac{L_s}{4\mu_o}(R_s^2 - R_m^2)\sum_{n=0}^{\infty} B_{nN_L}G_{nN_L}\left(-\frac{\cos(nN_L\alpha)}{2}[2\pi - 0] + \frac{1}{2}\left[\begin{pmatrix}\cos(nN_L\alpha)\cdot\dfrac{\sin(2nN_L\theta)}{2nN_L}\\ +\sin(nN_L\alpha)\cdot\left(\dfrac{-\cos(2nN_L\theta)}{2nN_L}\right)\end{pmatrix}\right]_0^{2\pi}\right)$$

$$= \frac{L_s}{4\mu_o}(R_s^2 - R_m^2)\sum_{n=0}^{\infty} B_{nN_L}G_{nN_L}\left(-\pi\cos(nN_L\alpha) + \frac{1}{2}\begin{bmatrix}\cos(nN_L\alpha)\cdot(0) - \sin(nN_L\alpha)\cdot(1)\\ -\left(\dfrac{\cos(nN_L\alpha)}{2}.0\right) + (\sin nN_L\alpha\cdot(1))\end{bmatrix}\right)$$

Finally

$$W(\alpha) = -\frac{L_s}{4\mu_o}(R_s^2 - R_m^2)\sum_{n=0}^{\infty} B_{nN_L}G_{nN_L}\pi\cos(nN_L\alpha) \tag{9}$$

Substituting Eq. (9) in Eq. (1) we get,

$$\begin{aligned} T_{cog} &= -\frac{\partial W(\alpha)}{\partial\alpha}\\ &= \frac{\partial}{\partial\alpha}\left(\frac{\pi L_s}{4\mu_o}(R_s^2 - R_m^2)\sum_{n=0}^{\infty} B_{nN_L}G_{nN_L}\cos(nN_L\alpha)\right)\\ &= \frac{\pi L_s}{4\mu_o}(R_s^2 - R_m^2)\cdot\frac{\partial}{\partial\alpha}\left(\sum_{n=0}^{\infty} B_{nN_L}G_{nN_L}\cos(nN_L\alpha)\right)\\ &= \frac{\pi L_s}{4\mu_o}(R_s^2 - R_m^2)\cdot\left(\sum_{n=0}^{\infty} B_{nN_L}G_{nN_L}(-\sin(nN_L\alpha)\cdot nN_L)\right)\\ &= -\frac{\pi L_s}{4\mu_o}(R_s^2 - R_m^2)\cdot\left(\sum_{n=0}^{\infty} B_{nN_L}G_{nN_L}nN_L\sin(nN_L\alpha)\right) \end{aligned} \tag{10}$$

where G_{nNL} is the air gap permeance functions, and B_{nNL} is the flux density functions.

In Equation (10), B_{nN_L} and G_{nN_L} are unknown parameters and can be obtained from the proposed T-shaped bifurcated slots which are shown in Figures 2 and 3. The air gap permeance function G_{nNL} for the T-shaped bifurcation slots is derived with the help of Figure 2.

The air gap permeance function G_{nN_L} is shown below

$$G_{nN_L} = \frac{N_s}{\pi}\int_{-\frac{\pi}{N_s}-\frac{a}{2}}^{-\frac{\pi}{N_s}-\frac{b}{2h1}-\frac{c}{2h2}}\cos(nN_L\theta)\cdot d\theta + \int_{\frac{\pi}{N_s}+\frac{b}{2h1}+\frac{c}{2h2}}^{\frac{\pi}{N_s}+\frac{a}{2}}\cos(nN_L\theta)\cdot d\theta$$

$$= \frac{N_s}{\pi}\left[\frac{\sin(nN_L\theta)\cdot d\theta}{nN_L}\right]_{-\frac{\pi}{N_s}-\frac{a}{2}}^{-\frac{\pi}{N_s}-\frac{b}{2h1}-\frac{c}{2h2}} + \left[\frac{\sin(nN_L\theta)\cdot d\theta}{nN_L}\right]_{\frac{\pi}{N_s}+\frac{b}{2h1}+\frac{c}{2h2}}^{\frac{\pi}{N_s}+\frac{a}{2}}$$

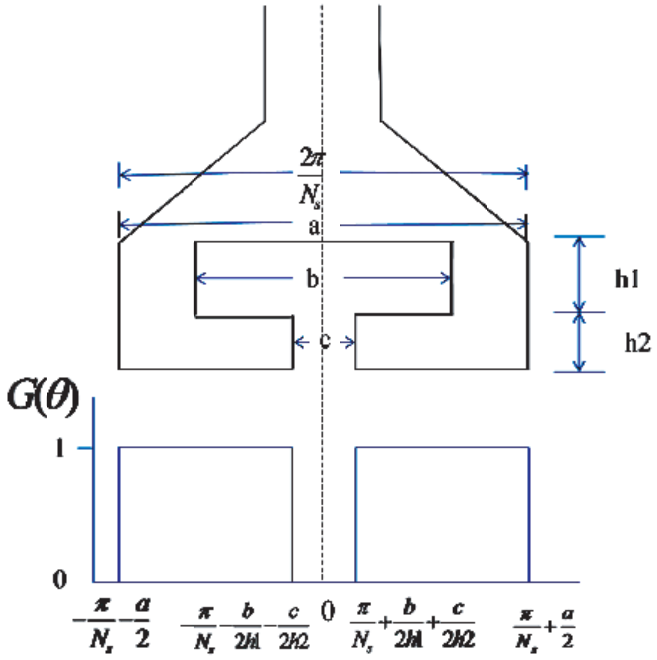

Figure 2. Simplified air gap permeance function for single stator slot.

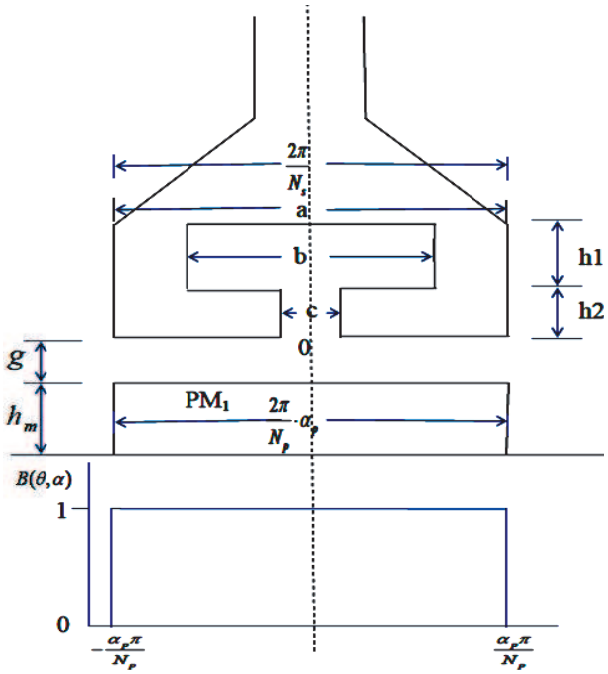

Figure 3. Simplified flux density functions for stator slot and rotor pole.

$$= \frac{N_s}{\pi n N_L}\left(\left[\sin\left(nN_L\left(-\frac{\pi}{N_s}-\frac{b}{2h1}-\frac{c}{2h2}+\frac{\pi}{N_s}+\frac{a}{2}\right)\right)\right]+\left[\sin\left(nN_L\left(\frac{\pi}{N_s}-\frac{b}{2h1}-\frac{c}{2h2}+\frac{\pi}{N_s}+\frac{a}{2}\right)\right)\right]\right)$$
$$= \frac{N_s}{\pi n N_L}\left(\left[\sin\left(nN_L\left(\frac{a}{2}-\frac{b}{2h1}-\frac{c}{2h2}\right)\right)\right]+\left[\sin\left(nN_L\left(\frac{a}{2}-\frac{b}{2h1}-\frac{c}{2h2}\right)\right)\right]\right)$$

Hence G_{nNL} is reduced to

$$G_{nN_L} = \frac{2N_s}{\pi n N_L}\left(\left[\sin\left(nN_L(\frac{a}{2}-\frac{b}{2h1}-\frac{c}{2h2})\right)\right]\right) \tag{11}$$

The flux density function B_{nNL} in rotor pole with respect to stator slot is derived using Figure 3. In the above Figure 3,
h_1 — depth of the inner (enlarged) bifurcated slot,
h_2 — depth of the outer (reduced) bifurcated slot,
g — length of air gap,
h_m — height of rotor magnetic pole above rotor and
α_p — Pole arc coefficient (defined as the ratio of axial length of the magnet to pole pitch).

The flux density function B_{nNL} is given by

$$= \frac{N_p B_\delta^2}{\pi}\left[\frac{\sin(nN_L(\theta-\alpha)}{nN_L}\right]_{-\frac{\alpha_p\pi}{N_p}}^{\frac{\alpha_p\pi}{N_p}}$$
$$= \frac{N_p B_\delta^2}{\pi n N_L}\left[\sin\left(nN_L\frac{\alpha_p\pi}{N_p}\right)+\sin\left(nN_L\frac{\alpha_p\pi}{N_p}\right)\right]$$
$$= \frac{N_p B_\delta^2}{\pi n N_L}\left[2\sin\left(nN_L\frac{\alpha_p\pi}{N_p}\right)\right]$$
$$= \frac{2N_p B_\delta^2}{\pi n N_L}\left[\sin\left(\frac{nN_L\alpha_p\pi}{N_p}\right)\right] \tag{12}$$

3. FLUX PLOTS IN T-SHAPED BIFURCATED STATOR SLOTS

The reluctance variation on change in flux density of the stator slots is the main reason for the cogging torque. Estimating the flux lines and the flux density functions are the two steps involved in the post-processing stage. The flux lines of T-shaped slot are nonuniform as compared to that of the reduced stator slot width. When applying the T-shaped bifurcation in reduced stator slot width, the flux density is lesser than the flux density of the normal reduced stator slot width motor. The flux lines and flux density plots for the Reduced Stator Slot width (Non-Bifurcated) and T-shaped Bifurcated slots are shown in Figures 4(a) and 4(b).

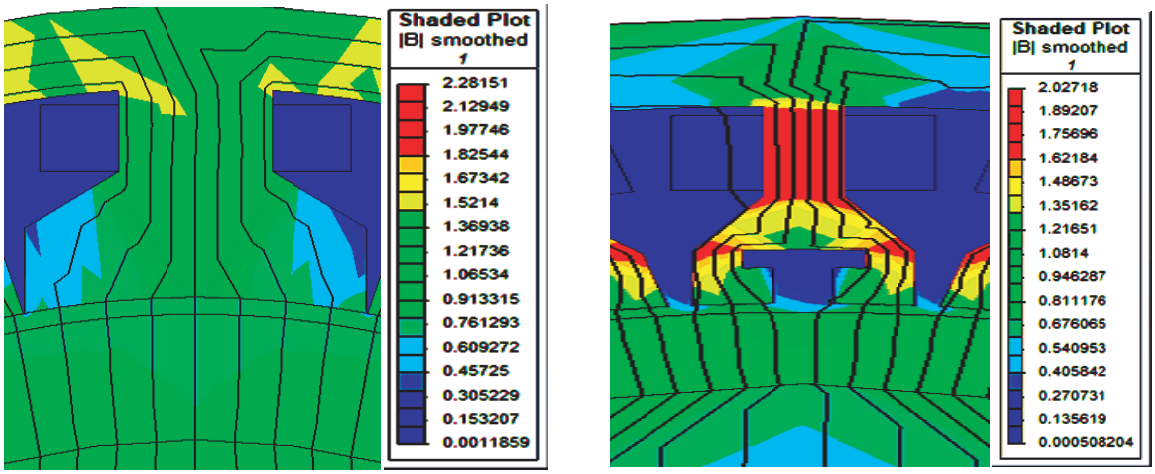

(a) (b)

Figure 4. Flux plots of BLDC motors for (a) reduced stator slot width and (b) T-shaped bifurcation of stator teeth.

When the stator slot opening is small, there is a change in the flux density distribution. Though the flux density remains the same in many regions of the BLDC motor, the maximum flux density indicated by yellow color is attained in some parts of the stator (in addition to the permanent magnets). Red areas indicate undesirable high flux density and may result in hot spots that may damage the motor. By applying the Reduced Stator Slot Width, the slot opening is very small, and the probability of development of hot spots increases. Hence, the change in flux density and the development of hot spots must also be considered while the Reduced Stator Slot Width modifications are done to reduce the cogging torque. When applying the T-shaped bifurcation in the stator tooth, the flux density is decreased which makes the reluctance change comparatively better than the existing method and results in cogging torque reduction. By modifying the shape of stator slots, it is found that the cogging torque is reduced for the proposed T-shaped bifurcation.

4. ANALYSIS OF RESULTS

This FEA is carried out for cogging torque reduction in BLDC motor by applying T-shaped bifurcation of stator slots. The FEA results are obtained analytically by applying VWM and also by simulation using CAD software. The cogging torque reduction found from the analytical results in T-shaped bifurcation is compared with the results obtained through CAD simulation. Both the CAD and FEA results of T-shaped Bifurcation in stator teeth are shown in Figure 5, and their cogging torque values are very close to each other. The performance comparisons of cogging torque and flux densities for existing and the proposed methods in stator slot modification techniques are given in Table 1 and also shown in Figure 6.

The analysis of results shows the performance of both existing and proposed techniques in stator

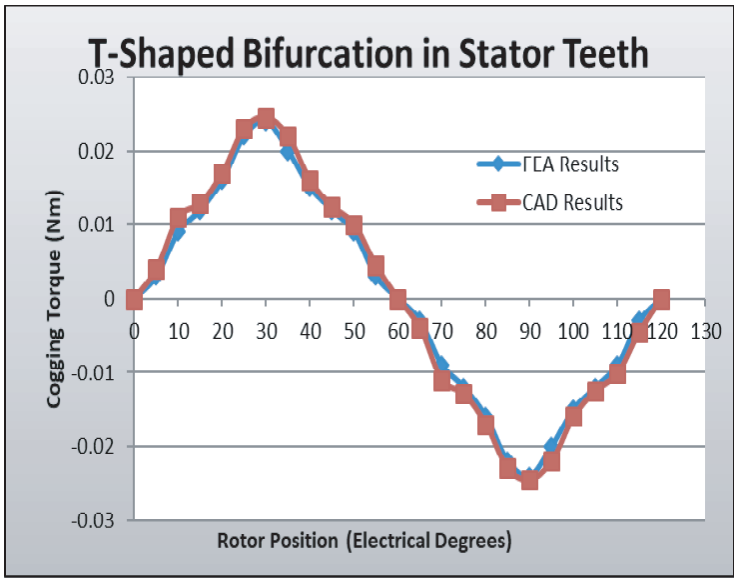

Figure 5. FEA and CAD results for T-shaped bifurcation in stator teeth.

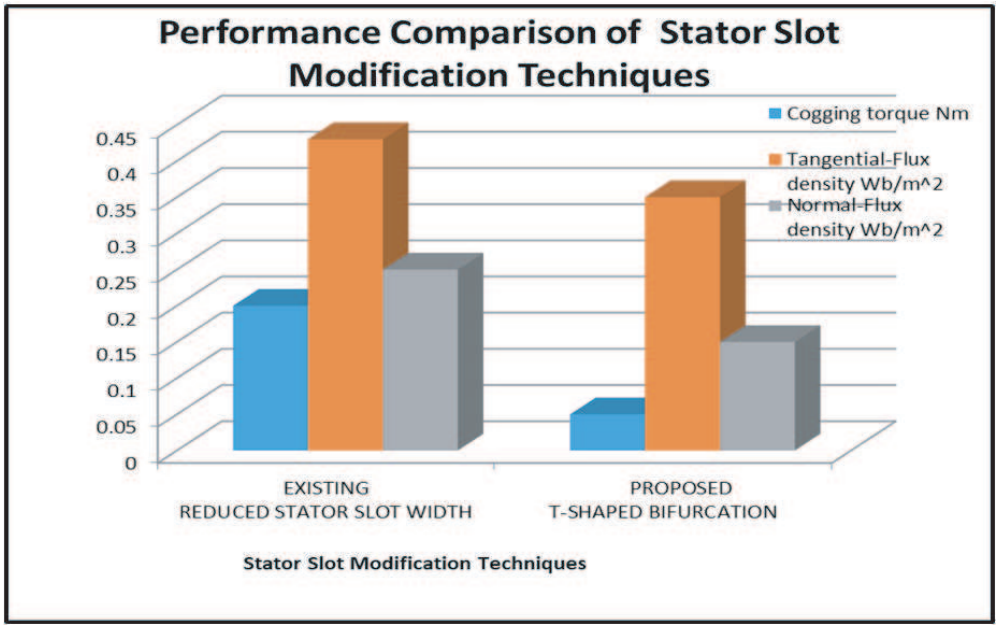

Figure 6. Performance comparisons of the stator slot modification techniques.

Table 1. Comparison of cogging torque and flux densities for stator slot modification techniques.

Prototypes	Tangential Flux density Wb/m^2	Normal Flux density Wb/m^2	Cogging Torque (Nm)	Torque (Nm)
Reduced Stator Slot Width	0.43	0.25	0.4	2.5
T-shaped Bifurcation	0.35	0.10	0.05	1.8

slot modification. From Figure 6, the peak to peak value of cogging torque is 0.4 Nm in reduced stator slot width techniques. When applying the T-shaped bifurcation in stator tooth, the cogging torque is reduced from 0.4 Nm to 0.05 Nm. The cogging torque is reduced up to 87.5% in the proposed T-shape bifurcation technique compared to existing reduced stator slot width technique. The reduction of cogging torque may also reduce the mechanical torque, frictional losses and air gap flux of the motor [13]. When the mechanical loss is reduced, the efficiency and life time performance of motor are improved. The speed is achieved up to 4000 rpm. The torque range is clearly shown in the performance of proposed T-shaped bifurcated BLDC motor characteristics, shown in Figure 7.

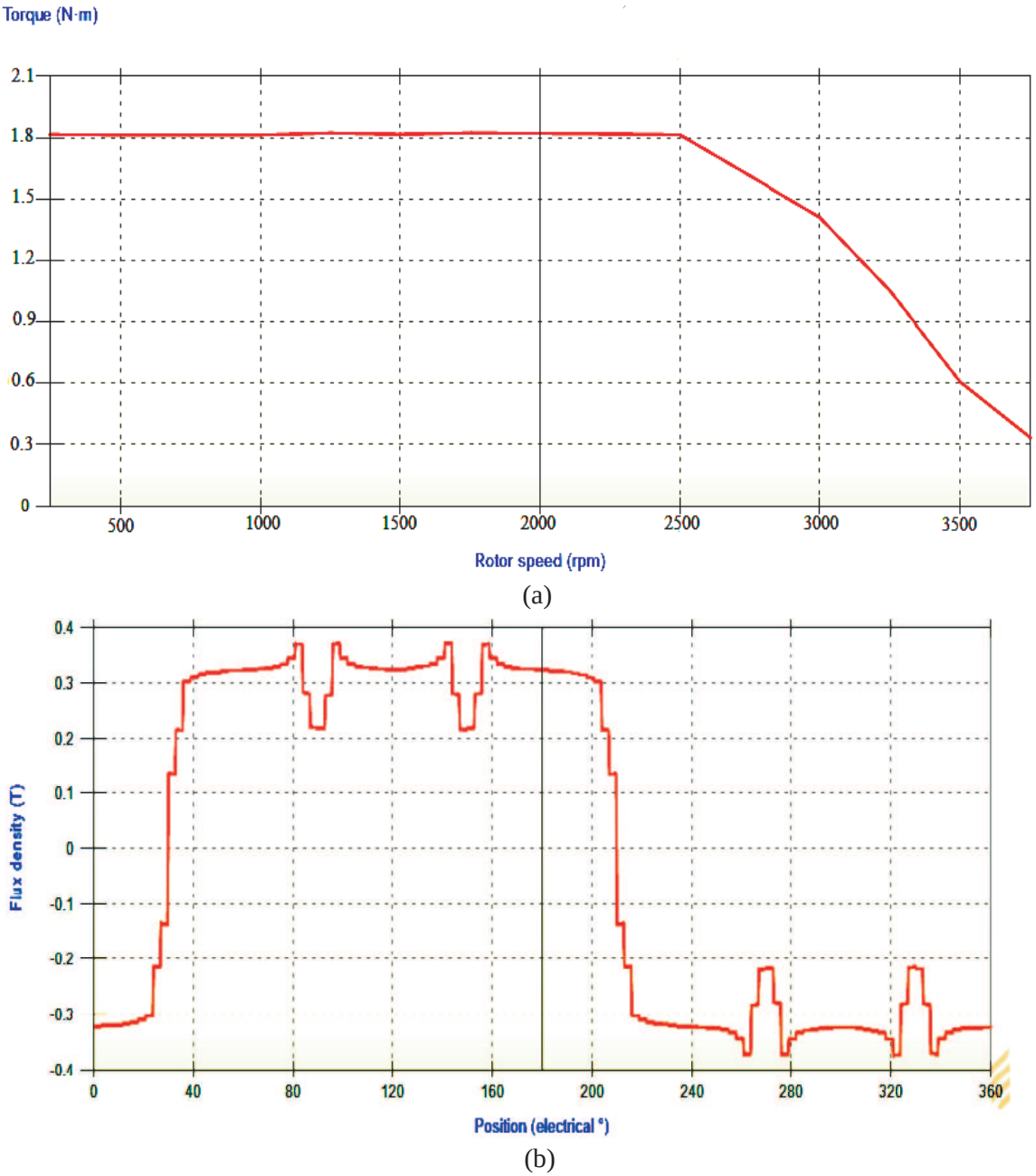

Figure 7. Performance of proposed T-shaped bifurcated BLDC motor. (a) Torque vs speed characteristics. (b) Air gap flux density.

5. CONCLUSION

In this paper, we propose a new method namely T-shaped bifurcation in stator teeth to reduce the cogging torque in radial flux surface mounted PMBLDC motor. The Finite Element Analysis (FEA) is carried out using Virtual Work Method (VWM) for the T-shaped bifurcation in stator teeth. The proposed method in this paper has been designed using CAD package MagNet software. FEA and CAD simulated results of cogging torque values for the PMBLDC motor are compared, and they are found to be nearly the same. Again the cogging torque and flux density of the motor calculated using the proposed T-shaped bifurcation method are compared with the existing Reduced Stator Slot Width method. From the performance results, the proposed T-shaped bifurcation yields much reduced cogging torque as compared to the existing and bifurcation techniques in stator slots.

REFERENCES

1. Islam, M. S., S. Mir, and T. Sebastian, "Issues in reducing the cogging torque of mass-produced permanent-magnet brushless DC motor," *IEEE Trans. Ind. Applicat.*, Vol. 40, 813–820, May/Jun. 2004.
2. Arun Noyal Doss, M., S. Jeevananthan, S. S. Dash, and J. Hussain, "Critical evaluation of cogging torque in BLDC motor for various techniques," *International Journal of Automation and Control*, Vol. 7, No. 3, 135–146, Sep. 2013.
3. Shin, P. S., S. H. Woo, Y. Zhang, and C. S. Koh, "An application of Latin hypercube sampling strategy for cogging torque reduction of large-scale permanent magnet motor," *IEEE Trans. Magn.*, Vol. 44, No. 11, 4421–4424, Nov. 2008.
4. Jiang, X., J. Xing, Y. Li, and Y. Lu, "Theoretical and simulation analysis of influences of stator tooth width on cogging torque of BLDC motors," *IEEE Trans. Magn.*, Vol. 45, No. 10, 4601–4604, Nov. 2008.
5. Lin, D., S. L.Ho, and W. N. Fu, "Analytical prediction of cogging torque in surface-mounted permanent-magnet motors," *IEEE Trans. Magn.*, Vol. 45, 3296–3302, Sept./Oct. 2009.
6. Saravanan, S., M. Arunnoyaldoss, S. Jeevananthan, and S. Vidyasagar, "Reduction of cogging torque by adapting semicircled permanent magnet," *ICEES 2011*, 2011.
7. Upadhyay, P. R. and K. R. Rajagopal, "FE analysis and CAD of radial-flux surface mounted permanent magnet brushless DC motors," *IEEE Trans. Magn.*, Vol. 41, 3952–3954, Sept./Oct. 2005.
8. Arun Noyal Doss, M., V. Ganapathy, V. Marthandan, and D. Mahesh, "Modeling and simulation of brushless DC motor for minimizing the cogging torque, harmonics and torque ripples," *International Review on Modelling and Simulation*, Vol. 6, No. 5, PART-A, 1452–1457, Oct. 2013.
9. Yang, Y., X. Wang, C. Zhu, and C. Huang, "Reducing cogging torque by adapting isodiametric permanent magnet," *IEEE Proc.-Electro.*, 2009.
10. Arun Noyal Doss, M., Md. Rizwan, and S. Jeevananthan, "Reduction of cogging torque in PMBLDC motor with reduced stator tooth width and bifurcated surface area using finite element analysis," *International Conference on Electrical Energy System at SSN*, 106–110, 2011.
11. Fazil, M. and K. R. Rajagopal, "Nonlinear dynamic modeling of a single-phase permanent-magnetbrushless DC motor using 2-D static finite-element results," *IEEE Trans. Magn.*, Vol. 47, No. 4, 781–786, Apr. 2011.
12. Wang, D., X. Wang, M.-K. Kim, and S.-Y. Jung, "Integrated optimization of two design techniques for cogging torquereduction combined with analytical method by a simple gradient descent method," *IEEE Trans. Magn.*, Vol. 48, No. 8, 2265–2276, Aug. 2012.
13. Yang, Y., X. Wang, C. Zhu, and C. Huang, "Reducing cogging torque by adapting isodiametric permanent magnet," *IEEE Proc.-Electro.*, 1028–1031, 2009.